Effects of CapG Overexpression on Agonist-induced Motility and Second Messenger Generation

Hui-Qiao Sun, Katarzyna Kwiatkowska, Dennis C. Wooten, and Helen L. Yin

The University of Texas Southwestern Medical Center, Department of Physiology, Dallas, Texas 75235-9040

Abstract. Actin modulating proteins that bind polyphosphoinositides, such as phosphatidylinositol 4, 5-bisphosphate (PIP_2), can potentially participate in receptor signaling by restructuring the membrane cytoskeleton and modulating second messenger generation through the phosphoinositide cycle. We examined these possibilities by overexpressing CapG, an actin filament end capping, Ca^{2+}- and polyphosphoinostide-binding protein of the gelsolin family. High level transient overexpression decreased actin filament staining in the center of the cells but not in the cell periphery. Moderate overexpression in clonally selected cell lines did not have a detectible effect on actin filament content or organization. Nevertheless, it promoted a dose-dependent increase in rates of wound healing and chemotaxis. The motile phenotype was similar to that oobserved with gelsolin overexpression, which in addition to capping, also severs and nucleates actin filaments. CapG overexpressing clones are more responsive to platelet-derived growth factor than control-transfected clones. They form more circular dorsal membrane ruffles, have higher phosphoinositide turnover, inositol 1,4,5-trisphosphate generation and Ca^{2+} signaling. These responses are consistent with enhanced PLCγ activity. Direct measurements of PIP_2 mass showed that the CapG effect on PLCγ was not due primarily to an increase in the PIP_2 substrate concentration. The observed changes in cell motility and membrane signaling are consistent with the hypothesis that PIP_2-binding actin regulatory proteins modulate phosphoinositide turnover and second messenger generation in vivo. We infer that CapG and related proteins are poised to coordinate membrane signaling with actin filament dynamics following cell stimulation.

THE discovery that some actin binding proteins are regulated by phosphatidylinositol 4,5-bisphosphate (PIP_2)[1] and their binding to PIP_2 modulates phosphatidylinositol-specific phospholipase C (PLC) activity in vitro raised the possibility of a reciprocal relation between regulations of the plasma membrane cytoskeleton and signaling (reviewed in Stossel, 1993). Among these, the gelsolin family and profilin are strong candidates. The gelsolin family of proteins (Yin, 1987; Weeds and Maciver, 1993) are activated by Ca^{2+} to sever and cap actin filaments. They are inhibited by polyphosphoinositides (Stossel, 1993) which can uncap gelsolin from filament ends to generate actin nuclei. Profilin, an actin monomer-binding protein which has complex effects on actin polymerization (Theriot and Mitchison, 1993; Sohn and Goldschmidt-Clermont, 1994), dissociates from actin monomers in the presence of polyphosphoinositides to increase the pool of polymerization-competent actin monomers. It is therefore postulated that fluctuations in polyphosphoinositide concentration following cell activation transiently stimulate actin polymerization via gelsolin and profilin. In vitro data suggest that these actin regulatory proteins may in turn modulate membrane signaling. Profilin inhibits unphosphorylated PLCγ but not tyrosine-phosphorylated PLCγ (Goldschmidt-Clermont et al., 1990, 1991). Inhibition by profilin is likely to be due to sequestration of the common substrate PIP_2, and can explain why the PLCγ activity in cell lysates is higher than in intact quiescent cells (Margolis et al., 1990). Gelsolin also inhibits unphosphorylated PLCγ (Banno et al., 1992), but its effect on tyrosine-phosphorylated PLCγ has not been examined.

Overexpression studies are consistent with the possibility that gelsolin and profilin regulate cell motility (Cunningham et al., 1991; Finkel et al., 1994). However, because these proteins have complex effects on actin, it is difficult to pinpoint the precise mechanism which accounts for the observed changes in cell motility and actin structures. Furthermore, the question of whether phosphoinositide signaling

CapG is a new nomenclature for a protein referred to previously as gCap39 (Yu et al., 1990), macrophage capping protein (Southwick and DiNubile, 1986), or mbh1 (Prendergast and Ziff, 1991). The new name is adopted because cDNA and genomic analyses showed that they are identical.

Address all correspondence to Helen L. Yin, The University of Texas Southwestern Medical Center, Dept. of Physiology, 5323 Harry Hines Blvd., Dallas TX 75235-9040. Tel.: (214) 648-7967. Fax: (214) 648-8685.

1. *Abbreviations used in this paper*: Ctrl, control clones; gK, CapG overexpressing lines; IP_3, inositol 1,4,5-trisphosphate; p, confidence internal; PDGF, platelet-derived growth factor; PIP_2, phosphatidylinositol 4,5-bisphosphate; PLC, phospholipase C.

was altered by overexpression of polyphosphoinositide binding proteins was not examined.

In this study, we overexpressed the simplest PIP_2-binding member of the gelsolin family to determine its effect on cell motility and second messenger generation. This protein, CapG (see footnote), caps actin filament without severing and does not bind actin monomers (Young et al., 1990; Yu et al., 1990, 1991). It is therefore strictly an actin capping protein. CapG overexpression, like gelsolin overexpression, increased cell locomotion in a dose-dependent manner. It also enhanced membrane ruffling in response to platelet-derived growth factor (PDGF), increased phosphoinositide turnover, inositol 1,4,5-trisphosphate (IP_3) generation and Ca^{2+} signaling. These results suggest that CapG potentiates signaling through the phosphoinositide cycle, and identify enhanced PLCγ activity as a possible mechanism.

Materials and Methods

Cell Culture and Transfection

The mouse CapG cDNA (Yu et al., 1990) was subcloned into pCMV3, which has a cytomegalovirus promoter and was transfected into monkey CV1 fibroblasts using DEAE-dextran as described (Yu et al., 1994) for transient expression. Cells were analyzed 2 d after transfection.

For stable expression, CapG cDNA was inserted through the BamHI/HindIII sites into the β-actin promoter driven expression vector LK588 (Gunning et al., 1987), which contains a neomycin resistance gene. NIH3T3 cells maintained in DME supplemented with 10% fetal calf serum were transfected by incubating with 20 μg expression vector and 60 μg lipofectin (GIBCO BRL, Gaithersburg, MD) in 2.8 ml OPTI-MEM I (GIBCO BRL) (per 100-mm plate) for 5 h. Cells were incubated in DME/10% FBS for 18 h, and were then exposed to 1 mg/ml G418 (geneticin; GIBCO RL). Resistant clones were selected after two weeks. Control clones (Ctrl) were transfected with the vector without a CapG cDNA insert.

Immunoblotting

Cells were lysed in cold RIPA buffer (50 mM NaCl, 0.1% SDS, 1% NP40 2 mM EDTA, 2 mM EGTA, 50 mM Hepes, pH 7.4) containing 2 mM PMSF and 2 μg/ml each of aprotinin, leupeptin, and pepstatin. Lysate protein concentrations were determined by the micro BCA method (Pierce Chem. Co., Rockford, IL). Proteins were electrophoresed on 5–20% polyacrylamide, discontinuous pH slab gels in the presence of SDS, and then transferred to nitrocellulose filters. They were probed with rabbit anti-mouse CapG and in some cases, simultaneously with rabbit anti-mouse gelsolin (Onoda et al., 1993). Immunoreactive bands were visualized with the ECL detection system (Amersham Corp., Arlington Heights, IL). Blots were exposed to x-ray films and the intensity of the immunoreactive bands was determined by scanning with a densitometer (300A; Molecular Dynamics, Sunnyvale, CA). Some samples were also blotted with a monoclonal anti-actin (Boehringer Mannheim Corp., Indianapolis, IN) and polyclonal anti-profilin (made in this laboratory). The sample load was within the linear range of the assay, as determined by analyzing a range of standard protein concentrations (Onoda et al., 1993).

Immunoprecipitation

NIH3T3 cells were labeled with [^{35}S]-TransLabel (0.2 mCi/ml; ICN Biomedical, Inc., Irvine, CA) for 6 h and lysed in RIPA buffer containing protease inhibitors. CapG was immunoprecipitated with affinity-purified rabbit anti-CapG and IgGsorb (New England Enzyme Center, Cambridge, MA) (Onoda and Yin, 1993). The immune complexes were analyzed by SDS–polyacrylamide gel electrophoresis. Radioactive bands were detected by fluorography on preflashed x-ray films and quantitated by densitometry scanning.

Assays for Cell Motility

Two methods described in (Cunningham et al., 1991) were used. (*a*) Chemotaxis: migration of cells through a 5-μm polycarbonate filter in a modified 48-well Boyden chamber (Nucleopore, Pleasanton, CA). The 5 × 10^4 cells (in 50 μl) were loaded in the top wells (three randomly selected wells per determination) and 28 μl medium containing no FCS or 10% FCS was added to the bottom wells. After 3–6 h, at 3°C, the filter separating the two chambers was fixed and stained with Diff-Quik (Baxter, McGaw Park, IL). Stained cells, which migrated through the filter were scored under a 20× microscope objective. (*b*) Wound healing: migration of cells to cover a "wound" made by scratching a ~1-mm line in a confluent monolayer. At hourly intervals, the width of the wound was measured at the same location using a 20× microscope objective, with a grid reticule in the eye piece. The rate of migration was determined from the slope of the plot of the distance traveled by the wound edge per h, and expressed as μm/h.

Fluorescence Microscopy

NIH3T3 cells were starved in DME/0.2% serum for 24 h and in a completely defined 1:1 DME/F12 medium supplemented with 20 mM Hepes, pH 7.4, 0.5 mg/ml BSA, 1 μg/ml insulin, and 1 μg/ml transferrin (Sigma Chem. Co., St. Louis, MO) (Q-medium) for an additional 18 h. They were stimulated with 70 ng/ml PDGF (AB chains; UBI, Lake Placid, NY) in Q medium at 37°C. Cells were fixed with 3% paraformaldehyde in PHEM buffer (60 mM Pipes, 25 mM Hepes, 10 mM EGTA, 4 mM $MgCl_2$, pH 6.9) for 30 min at room temperature, quenched with 50 mM NH_4Cl for 10 min, permeabilized with ice-cold 0.1% Triton X-100 for 7 min and labeled with 1 μg/ml tetramethyl rhodamine isothiocyanate phalloidin (rhodamine-phalloidin) (Sigma Chem. Co.) for 1 h. Coverslips were mounted in moviol supplemented with DABCO, and examined with 40× oil immersion objectives under a Zeiss Axiovert fluorescence microscope (Carl Zeiss, Inc., Thornwood, NY).

CV1 cells were fixed and permeabilized as described above. They were stained with rhodamine-phalloidin and rabbit anti-CapG/FITC-secondary antibody. Cells were examined under a Zeiss Axiovert fluorescence microscope.

Actin filament contents in individual cells were quantitated by measuring their rhodamine phalloidin staining intensity. All observations were performed with a Zeiss Axiovert 135 inverted microscope with a 100S/NA 1.3 objective. Images were analyzed with the BDS Image Program (Image Analysis System, version 1.4.3) and were acquired with a cooled CCD camera under identical optical conditions. Neutral density filter 0.3 (50% transmission) and 1 s exposure were used to avoid saturation of the detection system. Each image on the screen encompassed 512 × 312 pixels (118 × 87 μm) and is processed by background subtraction. Contours of cells were carefully delineated and the area recorded. Integrated fluorescent intensities in defined areas were determined. Cells were chosen randomly from different fields, and those which overlapped with other cells were excluded.

Quantitation of Water-soluble Inositol Phosphates

Cells were labeled with [^{3}H]myo-inositol (3 μCi/ml) in DME/5% FCS for 48 h and in DME/0.5% FBS for another 24 h. They were stimulated with 50 ng/ml PDGF in the presence of 20 mM LiCl for timed intervals at 37°C, and extracted with 5% PCA (Sharpes and McCarl, 1982). The PCA-soluble supernatant was passed over a BioRad AG1-X8 columns (formate form) after neutralization with 1:1 tri-*n*-octylamine/freon. Total inositol phosphates (IP_T, sum of IP, IP_2, and IP_3) were eluted with 1.2 M ammonium formate and 0.1 M formic acid (Downes et al., 1986). Each point was performed in duplicate.

IP_3 Content

Serum-deprived cells (in Q-medium) were stimulated with PDGF or carrier. Inositol phosphates were extracted with an equal volume of a 5% perchloric acid solution containing 10 mM EDTA and 1 μM ATP. IP_3 content was assayed by competition with exogenous [^{3}H] IP_3 for binding to microsomes (Amersham assay kit). IP_3 standards were extracted and assayed under identical conditions.

PIP_2 Mass

The mass of PIP_2 was determined using the method of Chilvers (Chilvers et al., 1991). Lipids were extracted and hydrolyzed in 1 M KOH to convert PIP_2 to IP_3. The released IP_3 was quantitated using a competitive binding assay as described above and PIP_2 mass was calculated based on the formula provided by Amersham and normalized against total cell proteins.

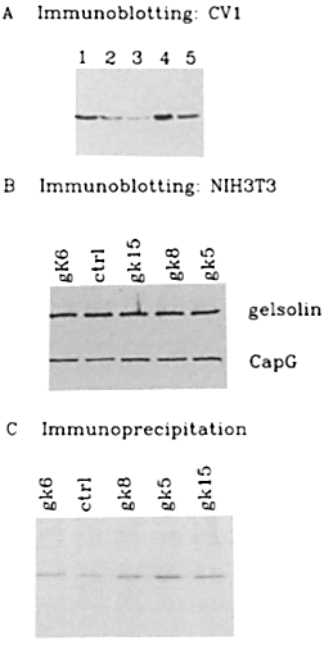

Figure 1. Analysis of CapG Overexpression. (A) Western blot of CV1 cells transiently transfected with pCMV Ctrl vector or pCMV-CapG. Lanes *1–3* and *5*, 2.5 and 1.25 μg of Ctrl cell extracts; lanes *4* and *5*, 1 and 0.5 μg of extracts obtained from cells transfected with CapG cDNA. Polypeptides were separated by SDS–polyacrylamide gel electrophoresis, blotted onto a nitrocellulose membrane, and probed with anti-CapG antibody. Immunoreactive bands were detected by enhanced chemiluminescence. (B) Western blot of NIH3T3 cells with stable CapG overexpression. 2 μg each of cells stably transfected with LK588 control vector (*Ctrl*) or LK588 with CapG cDNA insert (gK clones) were immunoblotted simultaneously with anti-CapG and anti-gelsolin. (*C*) Immunoprecipitation of CapG from stably transfected NIH3T3 cells. Lysates prepared from [^{35}S]-labeled Ctrl and CapG overexpressing cells were incubated with anti-CapG antibody, and CapG immune complexes were precipitated by adding a secondary antibody and IgGsorb. Radiolabeled CapG was analyzed by SDS-PAGE and detected by fluorography.

Intracellular Ca^{2+} Measurements

Cell monolayers starved in Q-medium were washed three times with buffer R (140 mM NaCl, 1 mM $MgCl_2$, 5 mM KCl, 10 mM Hepes, pH 7.4, 1 mM $CaCl_2$) and incubated with fura 2 (2 μM in the presence of 0.04% (wt/vol) pluronic-127 for 1 h at room temperature) in buffer R containing 1 mg/ml BSA and 2 mg/ml glucose. Cells were trypsinized briefly and proteolysis was stopped by adding threefold excess soybean trypsin inhibitor units. They were washed and resuspended in buffer R contaning BSA and glucose. Fluorescence measurements were performed with 4×10^7 cells in 1.5 ml with slow stirring, at excitation and emission wavelengths of 340 and 500 nm, respectively. $[Ca^{2+}]_i$ concentration was calibrated by addition of 1 mM $CaCl_2$ and 10 mM EGTA (pH 8.5) to obtain F_{max} and F_{min}, respectively, and assuming a K_dCa^{2+} of 224 nM, as described in (Minta et al., 1989).

Results

Transient Overexpression of CapG

CV1 cells transfected with pCMV-CapG had very high level CapG overexpression. Fig. 1 *A* compared the amount of CapG in CV1 cells transfected with ctrl vector or CapG cDNA by Western blotting. Densitometry scanning showed that the extent of overexpression for the entire cell population was between 5–10-fold. The extent of overexpression on a per cell basis would be much higher, since only 20–30% of the cells were transfected (based on increased CapG immunofluorescence, see below). For example, assuming that 20% of the cells were transfected, that CapG was uniformly overexpressed in the transfected cells, and the overexpression level for the entire cell population was fivefold, then each transfected cell would have 25-fold higher expression compared with untransfected cells.

High level overexpression was confirmed by brighter immunofluorescence staining with anti-CapG. Fig. 2 *A* shows a cell with increased CapG staining in the nucleus and cytoplasm. This is consistent with the nuclear and cytoplasmic distribution of CapG (Onoda et al., 1993). Although the surrounding cells contained endogenous CapG, the short exposure used to take the photographs detected low level staining in the nucleus but not in the cytoplasm. Cell shape was not noticeably altered.

The effects of CapG overexpression on actin filaments were determined by staining simultaneously with rhodamine phalloidin (Fig. 2 *B*). Normal CV1 fibroblasts had many actin stress fibers which crisscrossed the entire cell. Within the same field, the cell overexpressing CapG had decreased actin staining in the center, but still had significant staining of cortical actin filaments that are predominantly circumferential. Higher level overexpression (based on CapG staining, Fig. 2, *C* and *E*) resulted in almost complete loss of central actin staining and appearance of phalloidin-stained dots (Fig. 2, *D* and *F*). The circumferential actin filaments remained very prominent, and in some cases appeared to be more pronounced than in Ctrl cells.

While the transient expression results showed that CapG disrupted actin filament organization, we were not able to use this system to determine if cell motility or inositol lipid metabolism was altered because only a low percentage of cells was transfected and their CapG content was heterogenous and could not be quantitated reliably.

Stable Overexpression of CapG

These difficulties were overcome by using clonal cell lines which overexpressed defined levels of CapG. NIH3T3 cells were transfected with an expression vector containing a neo gene, and transfected cells were clonally selected. Ctrl NIH3T3 cells expressed endogenous CapG and gelsolin (Fig. 1 *B*, *ctrl*). Quantitative Western blotting showed that CapG and gelsolin accounted for 0.04 and 0.08% of total proteins in NIH3T3 cells (approximately equimolar ratio, after adjusting for differences in their molecular weights). After cDNA transfection, many CapG overexpressing lines (gK cells) were isolated (Fig. 1 *B*). The levels of CapG overexpression, based on densitometer scanning of Western blots, were between 1.3–1.8-fold (Table I). Immunoblotting with anti-gelsolin (Fig. 1 *B*), anti-profilin and anti-actin (data not shown) showed that there was no detectable change in the level of these cytoskeletal proteins (data not shown). (data not shown).

Overexpression was confirmed by immunoprecipitation of metabolically labeled CapG. More ^{35}S-labeled CapG was immunoprecipitated from clones transfected with CapG cDNA than Ctrl (Fig. 1 *C*). The extent of overexpression, based on densitometry scanning of the fluorographs (Table I), agreed with values obtained by Western blotting. 2-D gel analysis of the immunoprecipitated CapG showed that Ctrl and gK5 had a similar isoelectric profile (data not shown). Since the CapG isoforms reflect differential phosphorylation and subcellular localization (Onoda and Yin, 1993), the similar isoform profile suggested that the overexpressed CapG was not preferentially phosphorylated or compartmentalized compared with endogenous CapG.

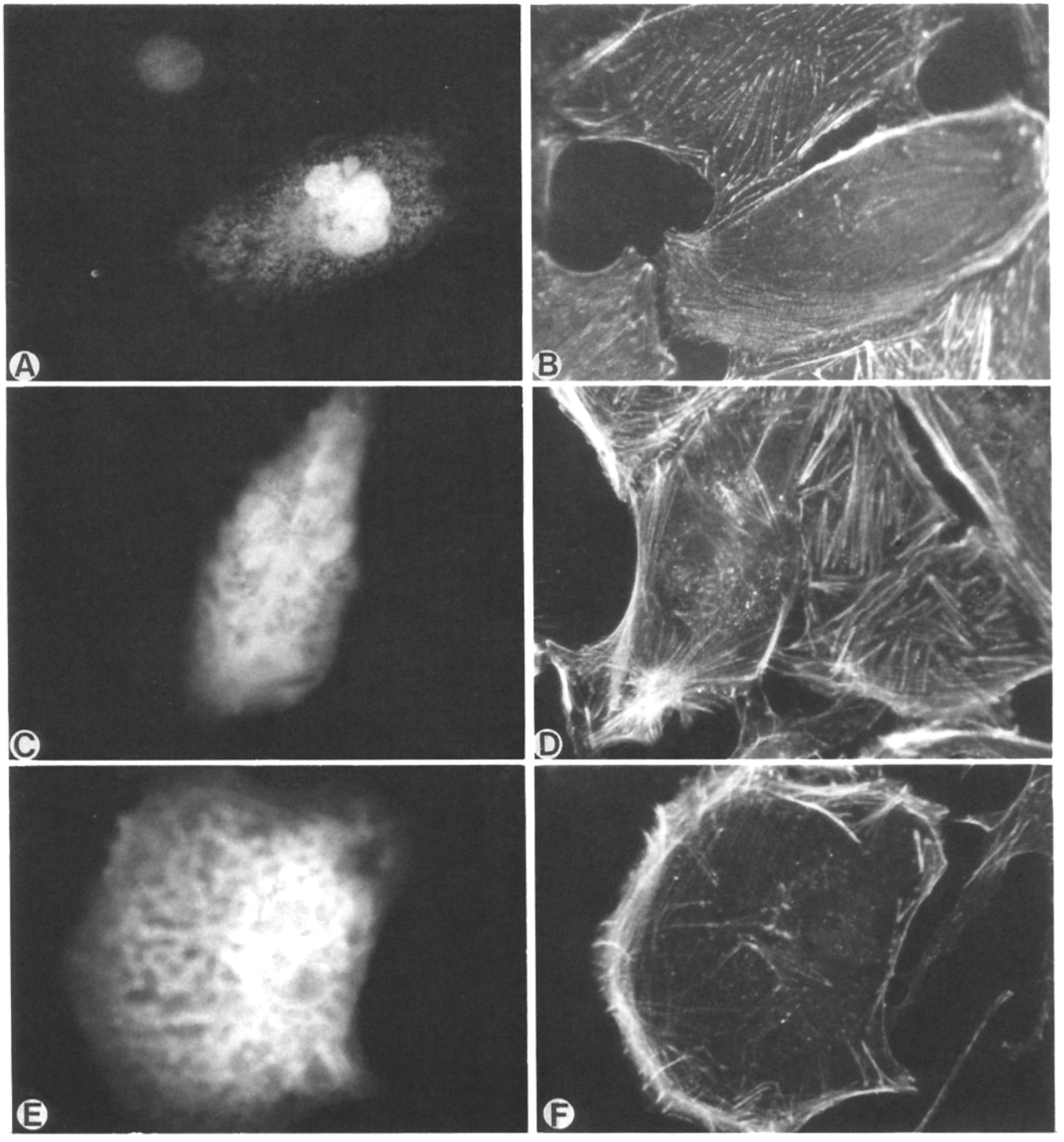

Figure 2. Effects of CapG overexpression on actin filaments in CV1 cells. Two days after completion of transfection with pCMV-CapG, cells were fixed, permeabilized, and stained with rabbit anti-CapG, FITC-anti IgG and rhodamine phalloidin. Cells were examined under a Zeiss Axiovert fluorescence microscope. (*A* and *B*, *C* and *D*, *E* and *F*) Paired images stained with anti-CapG and phalloidin, respectively.

We were not able to isolate stable cell lines with much higher than twofold overrexpression after three separate rounds of transfection with the LK588-CapG vector. The pCMV-CapG vector (driven by the CMV promoter instead of the β-actin promoter) which gave very high level overexpression in transient transfection studies also did not yield cells with high level expression after clonal selection. We suspect that although the cells tolerated CapG overexpression on the short term, high level overexpression was deleterious in the long term. A similarly low level of overexpression was reported for gelsolin overexpression clones (Cunningham et al., 1991).

Table I. Effects of CapG Overexpression on Cell Motility

Cell line	Fold CapG Overexpression*		Motility‡	
	Western Blotting (n = 4)	Immppt. (n = 2)	Chemotaxis (no. of cells)	Migration
				$\mu m/h$
Ctrl	1	1	31.4 ± 4.2 (n = 56)	11.1 ± 0.42
gK6	1.3 ± .02	1.3	67.8 ± 16.1 (n = 18, $p < 0.05$)§	–
gK8	1.4 ± .02	1.5	76.1 ± 10.1 (n = 42, $p < 0.01$)	21.4 ± 0.53 (n = 5, $p < 0.001$)
gK15	1.5 ± .05	1.6	112.8 ± 24.8 (n = 18, $p < 0.01$)	24.4 ± 1.1 (n = 5, $p < 0.001$)
gK5	1.8 ± .08	2.1	146.5 ± 20.6 (n = 50, $p < 0.001$)	–

* CapG content was determined by computerized scanning of Western blots and fluorographs of immunoprecipitated [^{35}S]CapG similar to those shown in Fig. 1, and was expressed as a ratio to Ctrl. The intensity of the CapG bands was within the linear range of the assays. Values for CapG radioactivity for duplicate determinations varied within 10%.
‡ Motility was determined by chemotaxis or wound healing assays. Values were mean ± SEM.
§ n, number of independent experiments. Each chemotaxis assay was performed in duplicate or triplicate. p, confidence interval based on Student's unpaired t test, comparing Ctrl cell line with each gK.

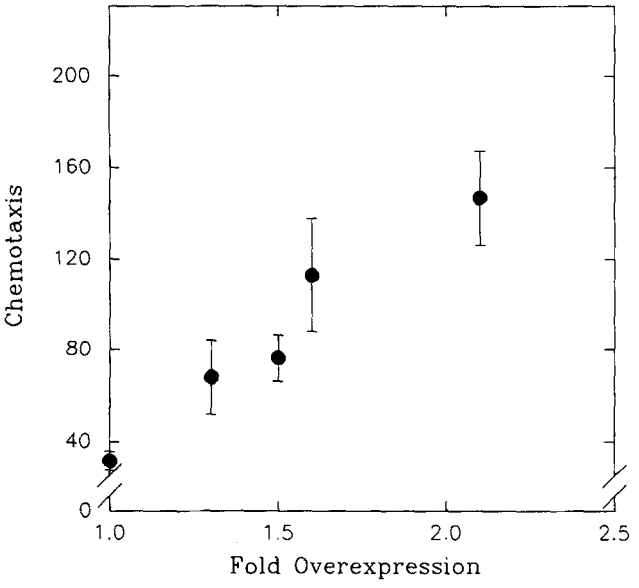

Figure 3. Relation between CapG overexpression and chemotaxis. The number of cells that migrated in a chemotactic chamber after 3 h in response to a serum gradient (10% in botom and 0% on top) was plotted as a function of CapG overexpression, based on the immunoprecipitation data shown in Table I. Chemotaxis values (number of cells migrated) are means ± SEM, n = 18–56, from Table I.

Motility of the Overexpressing Cell Lines

The CapG overexpressing cells translocated more rapidly than the Ctrl cells. Table I showed that in a chemotactic assay, 31 cells from a representative Ctrl line migrated through the filter in 3 h. Each of the gk clones studied exhibited a higher chemotactic response than Ctrl and the increase in motility was correlated with the extent of overexpression (Fig. 3). The difference between the pooled data from multiple experiments was statistically significant, with confidence intervals (p) of less than 0.05–0.001. Random motility, defined as migration in the absence of a serum gradient, was not increased significantly (data not shown).

Motility as measured by the rate of migration of cells into wounds in monolayers was also significantly higher in gk than Ctrl (Table I).

Cell Morphology and Membrane Ruffling in Response to PDGF Stimulation

The gk cell morphology and their actin stress fiber organization (revealed by rhodamine phalloidin staining) were not obviously different from Ctrl cells under normal culture conditions in 10% FCS (data not shown) and after serum deprivation (Fig. 4, *A* and *E*). Direct quantitation of rhodamine phalloidin intensity in individual cells confirmed that there was no significant difference in the amount of phalloidin stained actin (Table II). The CapG overexpressing cells were slightly larger, but the difference was not statistically significant (Table II).

A difference in the behavior of the cells was observed after PDGF treatment. Quiescent starved cells were very flat and contained thin actin stress fibers. On exposure to PDGF, Ctrl starved cells became less flat and developed many membrane ruffles. As described previously (Hedberg et al., 1993), two types of ruffles were observed: small lateral ruffles which were formed first and large circular folds on the dorsal surface (dorsal veils) which formed later (Fig. 4 *B, arrowheads*

Table II. Effects of CapG Overexpression on Actin Filament Content and Cell Area

Cell Line	Intensity*	Area‡
Ctrl	1140 ± 40	1824 ± 65
gK8	1208 ± 50	2080 ± 90

* Integrated intensity of rhodamine-phalloidin fluorescence, expressed in arbitrary units. 34 Ctrl and 26 gK8 cells were analyzed.
‡ Area of cell, in μm^2.

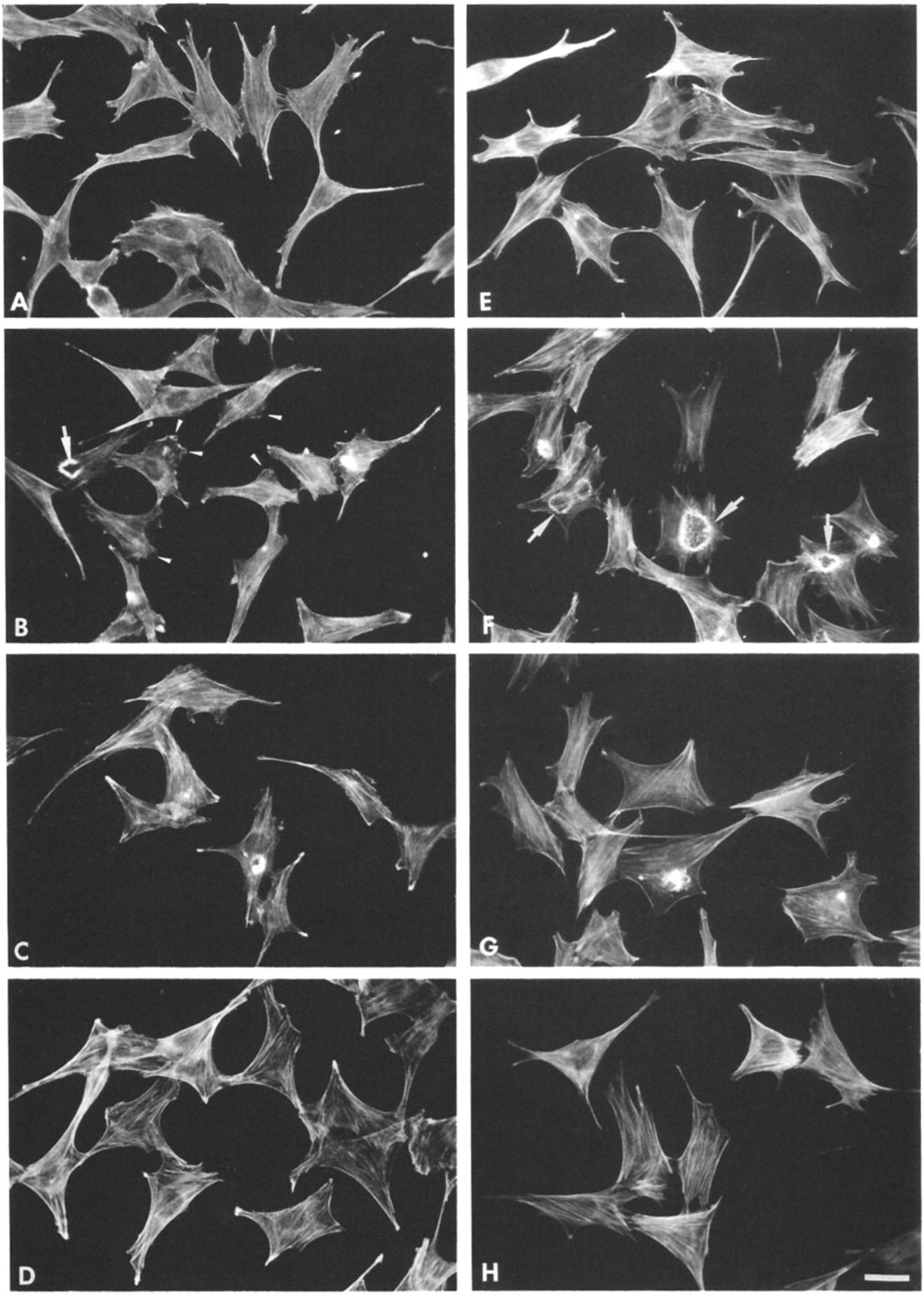
A
E
B
F
C
G
D
H

Table III. Effects of CapG Overexpression on Membrane Ruffling in Response to PDGF

Cell Line	Dorsal		Lateral		Dorsal and lateral	
	%*	Ratio	%*	Ratio	%*	Ratio
Ctrl 1	11.9	1.0	21.2	1.0	33.1	1.0
Ctrl 2	10.3	0.9	26.1	1.2	36.4	1.1
gK6	35.2	3.0	24.3	1.1	59.5	1.8
gK8	33.3	2.8	23.8	1.1	57.1	1.7

700–800 cells in 50 fields were examined per sample. Dorsal ruffles referred to large ring-like sheets of membrane on the dorsal surface; lateral ruffles referred to ruffles at the edge of the cell close to the substratum.
* Number of cells with ruffles per 100 cells. Ratio compared cells with ruffles in Ctrl 2, gK6, and gK8 with that of Ctrl 1.

and *arrow*, respectively). There was a loss of some actin stress fibers and appearance of dots of phalloidin-staining material. Dorsal ruffling was maximal by 5 min (Fig. 4 *B*) and subsided after 10 min (Fig. 4 *C*). gK6 had more dorsal ruffles compared with Ctrl. (Fig. 4 *F*). After 30 min, Ctrl and gK6 were indistinguishable: both were well spread and formed prominent stress fibers (Fig. 4, *D* and *H*).

The number of cells with lateral or dorsal ruffles was quantitated by scoring cells in multiple fields under a microscope (Table III). Two independently isolated Ctrl lines had similar ruffling activity (within 10–20%). In contrast, gK6 and gK8 nad approximately three times more cells with large dorsal ruffles, while the number of lateral ruffles was not changed compared with Ctrl.

Inositol Phosphate Levels

PDGF increases inositol lipid turnover and phosphorylates several important enzymes, including PLC which hydrolyzes PIP_2. Fig. 5 showed that PDGF induced a time-dependent increase in the amount of ^3H-labeled soluble inositol phosphates (IP_T) recovered from myo-inositol-labeled serum-deprived cells, and each of the gk clones generated more than Ctrl clones. Data pooled from several independent experiments showed that two Ctrl lines had similar IP_T, while the gK lines had highly significant increases in IP_T (Table IV).

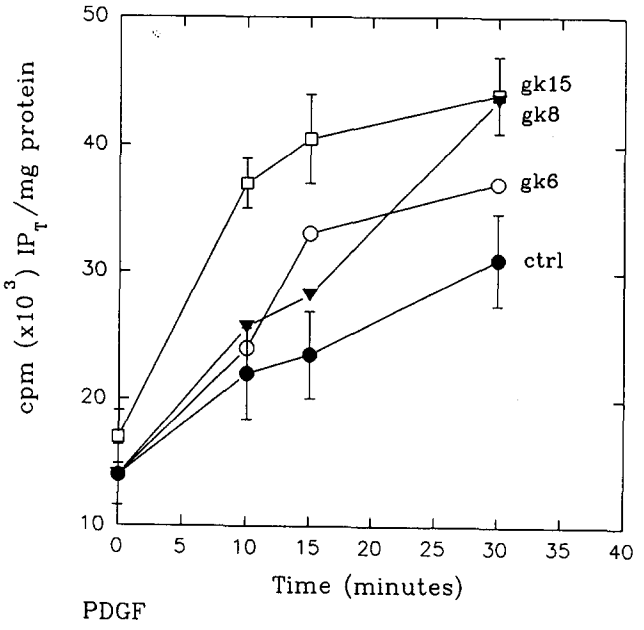

Figure 5. Effect of CapG overexpression on IP_T release after PDGF stimulation. Cells which were metabolically labeled with [^3H]myoinositol and serum-deprived were stimualted with 50 ng/ml PDGF in the presence of 20 mM LiCl for 0, 10, 15, and 30 min and were extracted with PCA. Soluble total inositol phosphates (IP_T) were recovered from anion exchange columns. Data shown were from a representative experiment. Each point was performed in duplicate, and the error bars indicated their range. Error bars for gK8 and gK6 (which are similar to those shown) were omitted for clearer presentation.

Table IV. Effect of CapG Overexpression on Total Inositol Phosphate (IP_T) Generation

Cell Line	Total inositol phosphates*		Ratio§
	Without PDGF	With PDGF	
Ctrl 1	14,022 ± 1,328 (n = 5)	28,576 ± 3,271 (n = 5)	2.0
Ctrl 2	15,344 ± 4,876 (n = 2)	29,592 ± 4,478 (n = 2)	1.9
gK8	14,657 ± 2,193 (n = 5)	37,500 ± 4,036 (n = 5, $p < 0.02$)‡	2.4
gK15	15,541 ± 4,362 (n = 3)	43,419 ± 4,825 (n = 4, $p < 0.01$)	2.8

Cells were stimulated with 50 ng/ml PDGF or carrier solution for 15 min at 37°C.
* IP_T expressed as mean ± SEM, in cpm/mg cell proteins.
‡ n, number of independent experiments, each performed in duplicate. p, confidence interval, based on Student's unpaired t test, between Ctrl 1 and each gK. Differences were not statistically significant in cases with no indicated p value.
§ Ratio was obtained by averaging the ratios of IP_T level in PDGF-treated vs. non-treated cells in paired experiments.

The effect of CapG overexpression on PLCγ activity per se was determined by quantitating IP_3, an immediate product of PIP_2 hydrolysis by PLC (Fig. 6). Control and CapG overexpressing cells had similar basal IP_3 level (~10 pmol/mg cell proteins). After stimulation with PDGF for 15 s, the IP_3 content of Ctrl cells increased to 16 pmol/mg protein, whereas that of CapG overexpressing clones increased to above 20 pmol/mg protein. The IP_3 level of the gk clones continued to be higher than Ctrl after 30 s of stimulation. Data from multiple experiments were summarized in Table V. Lines 1 and 2 were from paired experiments using Ctrl and gK8 cells. There was no significant difference in the

Figure 4. Effect of CapG overexpression on actin filament organization in response to PDGF stimulation. NIH3T3 cell lines transfected with ctrl or CapG vectors were serum-deprived and stimulated with 70 ng/ml PDGF. At various intervals, cells were fixed, permeabilized, and stained with rhodamine phalloidin. Coverslips were examined with a Zeiss Axiovert fluorescence microscope. (*A–D*) Ctrl cells, 0, 5, 10 and 30 min after PDGF stimulation; (*E–H*) gK8. Arrowheads, lateral ruffles; arrows, dorsal ruffles. Bar, 25 μm.

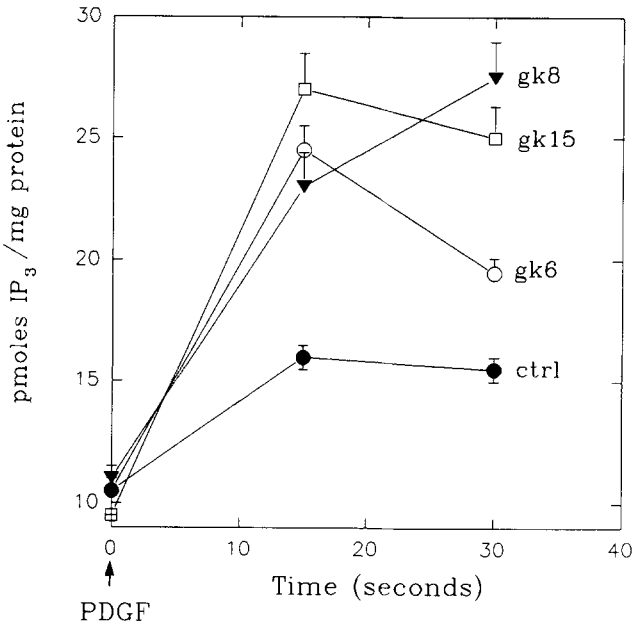

Figure 6. Effect of CapG overexpression on IP_3 generation in response to PDGF. Serum-deprived fibroblasts were stimulated with 100 ng/ml PDGF for 0, 15, and 30 s. Cells were extracted with PCA, and IP_3 level was determined by a receptor binding assay. Results shown were from a single representative experiment performed in triplicate. Values shown were mean ± SEM.

basal IP_3 content, but IP_3 level after PDGF stimulation was significantly higher in gK8 than Ctrl. This difference was not due to variability between clones because three other independently isolated Ctrl lines had a similar response to each other (line 3). Since PDGF activates PLCγ, our results suggested that overexpression of CapG enhanced PLCγ hydrolysis of PIP_2.

We compared the PIP_2 mass in cells to determine if increased PLCγ activity could be attributed to increased substrate concentration. Table V showed that there was no significant difference in the bulk PIP_2 mass of quiescent Ctrl and CapG overexpressing clones.

Ca^{2+} Signaling

Intracellular Ca^{2+} measurements with fura 2 showed that CapG overexpression altered Ca^{2+} homeostasis in a manner consistent with increased PDGF response (Fig. 7). Basal cytosolic Ca^{2+} levels for Ctrl and gK8 were 80.8 ± 3.5 and 83.1 ± 2.0 nM (mean ± SEM, n = 6–8), respectively. As described previously (Huang et al., 1991), PDGF induces a rise in $[Ca^{2+}]_i$ which decays slowly. This response is attributed to a combination of a transient IP_3-mediated Ca^{2+} release from internal stores and subsequent sustained Ca^{2+} entry from the extracellular medium. The initial peak Ca^{2+} in gK8 cells was consistently higher than that of Ctrl in paired experiments (240 ± 19.3 and 172.0 ± 12.4 nM, respectively, n = 6–8, $p < 0.05$), and the sustained phase was also increased.

Discussion

Overexpression of CapG in fibroblasts was used to investigate the effects of increased potential for actin filament end capping and polyphosphoinositide binding in vivo. Our data showed that CapG overexpression produced phenotypes which are consistent with perturbations of the actin cytoskeleton and membrane signaling.

Very high level overexpression (~25-fold) achieved by transient transfection, resulted in extensive actin depolymerization in the cell center. Excessive actin filament "barbed" end capping can cause depolymerization by blocking barbed end growth so there is net actin loss from the uncapped pointed ends. It has been reported previously that microinjection of a capping protein unrelated to CapG induces actin depolymerization in cells (Fuchtbauer et al., 1983). However, the amount of cortical actin filaments in the CapG overexpressing CV1 cells was not decreased, and in some cases, appeared to be increased. The lack of actin depolymerization in the cell periphery could be due to a number of factors and had been observed previously with overexpression of β-thymosin in CV1 cells (Yu et al., 1994) and profilin in CHO cells (Finkel et al., 1994). The peripheral actin filaments may be inherently more stable because they have a different actin isoform composition or are all protected by other stabilizing proteins. Another possibility is that CapG and/or additional regulatory proteins, such as profilin, are differentially active in the cell center compared with the cell periphery. Differential polymerization/depolymerization has been found in

Table V. Effects of CapG Overexpression on IP_3 and PIP_2 Levels

	No stimulus		PDGF	
Cell line	$[PIP_2]$	$[IP_3]$	$[IP_3]$	Ratio§
Ctrl	373 ± 20.7	8.9 ± 1.8	13.7 ± 2.1	1.5
gK8	385 ± 36.0	9.8 ± 1.7	25.8 ± 2.9 ($p < .001$)‡	2.6
Pooled Ctrl	–	10.6 ± 1.4	16.0 ± 1.5	1.5

Serum-deprived cells were stimulated with medium containing no addition or 100 ng/ml PDGF for 30 s at 37°C.
* $[IP_3]$, expressed as mean ± SEM in pmol/mg protein, from four to six independent experiments, each performed in triplicate. $[PIP_2]$, pmol/mg protein, from 7 (*Ctrl*) and 11 (*gK8*) independent experiments done in triplicate.
‡ Confidence interval, based on Student's unpaired t test, comparing PDGF-stimulated Ctrl results from a single cell line with gK8 or pooled Ctrl (results from four independently isolated Ctrl). Other differences with no indicated p values were not statistically significant.
§ Average $[IP_3]$ ratios between stimulated and unstimulated cells derived from paired experiment.

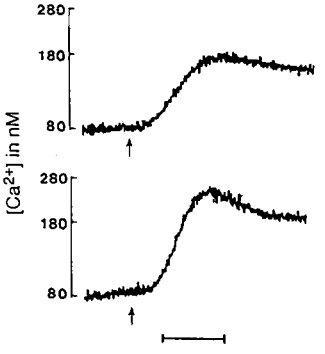

Figure 7. Effect of CapG overexpression on Ca^{2+} signaling in response to PDGF. Tracings from a representative experiment were shown. Bar, 1 min. Top, Ctrl; bottom, gK15. Arrows indicate time of PDGF addition.

many other systems. For example, when mast cells are stimulated with a secretagogue, there is selective actin depolymerization and polymerization in the cell periphery and center, respectively, due to differential activation of heterotrimeric and small GTP binding proteins (Normal et al., 1994). CapG is active at μM Ca^{2+} concentrations (Young et al., 1994) and when PIP_2 level is low. Furthermore, since CapG caps filaments reversibly (Yu et al., 1990), the consequences of uncapping should also be considered. Uncapping would release actin nuclei to promote polymerization, particularly when the actin monomer pool is expanded by stress fiber depolymerization (Carlier and Pantaloni, 1994; Sun et al., 1994).

Cell lines which stably overexpressed CapG at a much lower level did not have a detectable change in their actin filament content, based on analysis of rhodamine phalloidin staining. This is not unexpected, because the amount of overexpression was probably not sufficient to produce detectable changes in filamentous actin content and organization. Nevertheless, these cells have a recognizable phenotype that is consistent with alterations in the actin machinery and the signaling cascade: increased agonist-induced cell migration, enhanced response to PDGF, in terms of dorsal membrane ruffling, inositol phosphate release, IP_3 generation, and PLCγ activity.

Multiple controls were used to establish that these phenotypic changes were due to CapG overexpression and not artifacts of random gene integration and clonal selection. We analyzed a large number of control-transfected and CapG-transfected clones. Our independently isolated CapG clones have the same phenotype, and its severity is correlated with the level of CapG overexpression.

Curiously, the CapG effects on motility are similar to that of gelsolin overexpression (Cunningham et al., 1991). A priori, we would have predicted that gelsolin would be more potent because it can modify the actin cytoskeleton by severing as well as capping. Furthermore, it caps with higher affinity than CapG (apparent capping constant of 10 pM (Weeds and Maciver, 1993) instead of nM (Young et al., 1990; Yu et al., 1990; Dabiri et al., 1992), respectively. These considerations led us to suspect that the effects of overexpressing CapG are not determined solely by the increased availability of capping proteins, but may also be due to other common features which are amplified catalytically.

Enhanced generation of second messengers through the phosphoinositide pathway provides a plausible explanation for many of the observed phenotypic changes. In this scenario, CapG overexpression increased PDGF-induced phosphoinositide turnover and enhanced the hydrolysis of PIP_2 by PLCγ. This will increase the generation of a variety of important second messengers which can affect the motile responses directly or indirectly. We demonstrated that IP_3, an immediate product of PIP_2 hydrolysis, was increased. IP_3 promotes Ca^{2+} release from intracellular stores to activate Ca^{2+}-modulated proteins, including CapG. Although we did not measure diacylglycerol level, it is also likely to be increased. Diacylglycerol activates protein kinase C to phosphorylate a multitude of proteins and can induce actin polymerization via an actin nucleating protein in the membrane (Shariff and Luna, 1992). In this way, the small increase in CapG concentration can be amplified through at least two major signaling cascades. Hydrolysis of PIP_2 would also release and activate CapG, gelsolin and profilin to remodel the cytoskeleton.

The molecular mechanisms by which CapG overexpression enhances IP_3 generation have not yet been determined and are likely to be complex. Since CapG binds PIP_2 which is a substrate for PLCγ, one possibility is that CapG alters PLCγ activity by controlling the availability of PIP_2. This could occur either by increasing the total PIP_2 pool or compartmentalization of the pool to increase the local PIP_2 concentration or PIP_2 conformation. We were not able to detect a difference in the PIP_2 mass of serum-deprived Ctrl and CapG overexpressing cells. Therefore, the difference in PLC activity after PDGF stimulation is unlikely to be simply due to a change in the initial bulk PIP_2 concentration. However, since some cells have a substantial hormone-insensitive PIP_2 pool (Inokuchi and Imboden, 1990), it is not possible to rule out a small difference in the hormone-sensitive PIP_2 pool per se. Furthermore, local changes due to compartmentalization or aggregation of PIP_2 by binding to CapG cannot be assessed by bulk measurements. The latter possibility is supported by the finding that a PIP_2 binding peptide homologous to that identified in CapG and gelsolin (Janmey et al., 1992; Yu et al., 1992) increases PLC activity in vitro (Simoes et al., 1993). Alternatively, CapG may have a direct effect on PLC to increase its V_{max} or reduce K_m by binding to PLC. This mechanism is plausible since gelsolin and therefore possibly CapG binds to PLC (Banno et al., 1992).

Besides a direct effect on signal transduction, CapG may also exert an indirect effect by modifying the actin cytoskeleton to enhance the PDGF response. PLCγ activation is a complex process (reviewed in Rhee, 1991). The CapG effect can be exerted at the receptor level (dimerization, internalization, recycling), receptor/PLCγ/cytoskeletal association level, and at other unidentified interactive sites. Western blotting with antiphosphotyrosine antibody showed no obvious difference in the extent of tyrosine phosphorylation of major phosphorylated proteins, including the PDGF receptor (data not shown), so a direct effect on receptor kinase activation is not likely and the effects are probably exerted at a distal event. Additional experiments will be required to distinguish between a direct and indirect effect of CapG on signal transduction.

In conclusion, our results provided the first demonstration that a polyphosphoinositide-binding actin regulatory protein modulates inositol lipid metabolism in vivo and suggested a mechanism for linking membrane signaling with actin polymerization dynamics after receptor activation.

We thank S. Muallem for advice on fura-2 Ca^{2+} measurements, K. Luby-Phelps for advice on the imaging system, and F. X. Yu for initiating the transient transfection experiments.

This work was supported by National Institutes of Health grant GM51112 and The Welch Foundation.

Received for publication 14 April 1994 and in revised form 9 November 1994.

References

Banno, Y., T. Nakahima, T. Kumada, K. Ebisawa, Y. Nonomura, and Y. Nozawa. 1992. Effects of gelsolin on human platelet cytosolic phosphoinositide-phospholipase C isozymes. *J. Biol. Chem.* 267:6488–6494.

Carlier, M.-F., and D. Pantaloni. 1994. Actin assembly in response to extracellular signals: role of capping proteins, thymosin β_4 and profilin. *Sem. Cell Biol.* 5:183–191.

Chilvers, E. R., I. H. Batty, R. A. J. Challis, P. J. Barnes, and S. R. Nahorski. 1991. Determination of mass changes in phosphatidylinositol 4,5-bisphosphate and evidence for agonist-stimulated metabolism of inositol 1,4,5-trisphosphate in airway smooth muscle. *Biochem. J.* 275:373–379.

Cunningham, C. C., T. P. Stossel, and D. J. Kwiatkowski. 1991. Enhanced motility in NIH 3T3 fibroblasts that overexpress gelsolin. *Science (Wash. DC).* 251:1233–1236.

Dabiri, G. A., C. L. Young, J. Rosenbloom, and F. S. Southwick. 1992. Molecular cloning of human macrophage capping protein cDNA. *J. Biol. Chem.* 267:16545–16552.

Downes, C. P., P. T. Hawkins, and R. F. Irvine. 1986. Inositol 1,3,4,5-tetrakisphosphate and not phosphatidylinositol 3,4-bisphosphate is the probable precursor of inositol 1,3,4-trisphosphate in agonist-stimulated parotid gland. *Biochem. J.* 238:501–506.

Finkel, T., J. A. Theriot, K. R. Dise, G. F. Tomaselli, and P. J. Goldschmidt-Clermont. 1994. Dynamic actin structures stabilized by profilin. *Proc. Natl. Acad. Sci. USA.* 91:1510–1514.

Fuchtbauer, A., B. M. Jockusch, H. Maruta, M. W. Kilimann, and H. Isenberg. 1983. Disruption of microfilament organization after injection of F-actin capping proteins into living tissue culture cells. *Nature (Lond.).* 304: 361–364.

Goldschmidt-Clermont, P. J., L. M. Machesky, J. J. Baldassare, and T. D. Pollard. 1990. The actin-binding protein profilin binds to PIP_2 and inhibits its hydrolysis by phospholipase C. *Science (Wash. DC).* 247:1575–1578.

Goldschmidt-Clermont, P. J., J. W. Kim, L. M. Machesky, S. G. Rhee, and T. D. Pollard. 1991. Regulation of phospholipase C-γ1 by profilin and tyrosine phosphorylation. *Science (Wash. DC).* 251:1231–1233.

Gunning, P., J. Leavitt, G. Muscat, S. Y. Ng, and L. Kedes 1987. A human beta-actin expression vector system directs high-level accumulation of antisense transcripts. *Proc. Natl. Acad. Sci. USA.* 84:4831–4835.

Hedberg, K. M., T. Bengtsson, B. Safiejko-Mroczka, P. B. Bell, and M. Lindroth. 1993. PDGF and neomycin induce similar changes in the actin cytoskeleton in human fibroblasts. *Cell Motil. Cytoskeleton.* 24:139–149.

Huang, C.-L., T. Takenawa, and H. E. Ives. 1991. Platelet-derived growth factor-mediated Ca^{2+} entry is blocked by antibodies to phosphatidylinositol 4,5-bisphosphate but does not involve heparin-sensitive inositol 1,4,5-trisphosphate receptors. *J. Biol. Chem.* 266:4045–4048.

Inokuchi, S., and J. B. Imboden. 1990. Antigen receptor-mediated regulation of sustained polyphosphoinositide turnover in a human T cell line. Evidence for a receptor regulated pathway for production of phosphoinositol 4,5-bisphosphate. *J. Biol. Chem.* 265:5883–5889.

Janmey, P. A., J. Lamb, P. G. Allen, and P. T. Matsudaira. 1992. Phosphoinositide-binding peptides derived from the sequences of gelsolin and villin. *J. Biol. Chem.* 267:11818–11823.

Margolis, B., A. Zilberstein, C. Franks, S. Felder, S. Kremer, A. Ullrich, S. G. Rhee, K. Skorecki, and J. Schlessinger. 1990. Effect of phospholipase C-γ overexpression on PDGF-induced second messengers and mitogenesis. *Science (Wash. DC).* 248:607–610.

Minta, A., J. P. Y. Kao, and R. Y. Tsien. 1989. Fluorescent indicators for cytosolic calcium based on rhodamine and fluorescein chromophores. *J. Biol. Chem.* 264:8171–8178.

Norman, J. C., L. S. Price, A. J. Ridley, A. Hall, and A. Koffer. 1994. Actin filament organization in activated mast cells is regulated by heterotrimeric and small GTP-binding proteins. *J. Cell Biol.* 126:1005–1015.

Onoda, K., and H. L. Yin. 1993. gCap39 is phosphorylated. Stimulation by okadaic acid and preferential association with nuclei. *J. Biol. Chem.* 268: 4106–4112.

Onoda, K., F.-X. Yu, and H. L. Yin. 1993. gCap39 is a nuclear and cytoplasmic protein. *Cell Motil. Cytoskeleton.* 26:227–238.

Prendergast, G. C., and E. B. Ziff. 1991. Mbh1: a novel gelsolin/severin-related protein which binds actin in vitro and exhibits nuclear localization in vivo. *EMBO (Eur. Mol. Biol. Organ.) J.* 10:757–766.

Rhee, S. G. 1991. Inositol phospholipid-specific phospholipase C: interaction of the γ1 isoform with tyrosine kinase. *Trends Biochem. Sci.* 16:297–301.

Shariff, A., and E. J. Luna. 1992. Diacylglycerol-stimulated formation of actin nucleation sites at plasma membranes. *Science (Wash. DC).* 256:245–247.

Sharpes, E. S., and R. L. McCarl. 1982. A high-performance liquid chromatographic method to measure ^{32}P incorporation into phosphorylated metabolites in cultured cells. *Anal. Biochem.* 124:421–424.

Simoes, A. P., P. Schnabel, R. Pipkorn, M. Camps, and P. Gierschik. 1993. A peptide corresponding to a potential polyphosphoinositide binding site of phospholipase C-β_2 enhances its catalytic activity. *FEBS (Fed. Eur. Biochem. Soc.)* 331:248–251.

Sohn, R. H., and P. J. Goldschmidt-Clermont. 1994. Profilin: at the crossroads of signal transduction and the actin cytoskeleton. *Bioessays.* 16:465–472.

Southwick, F. S., and M. J. DiNubile. 1986. Rabbit alveolar macrophages contain a Ca^{2+}-sensitive, 41,000-dalton protein which reversibly blocks the "barbed" ends of actin filaments but does not sever them. *J. Biol. Chem.* 261: 14191–14195.

Stossel, T. P. 1993. On the crawling of animal cells. *Science (Wash. DC).* 260: 1086–1094.

Sun, H.-Q., K. Kwiatkowska, and H. L. Yin. 1995. Actin monomer binding proteins. *Curr. Opin. Cell Biol.* 7:102–110.

Theriot, J. A., and T. J. Mitchison. 1993. The three faces of profilin. *Cell.* 75: 835–838.

Weeds, A., and S. Maciver. 1993. F-actin capping proteins. *Curr. Opin. Cell Biol.* 5:63–69.

Yin, H. L. 1987. Gelsolin: calcium- and polyphosphoinositide-regulated actin-modulating protein. *Bioessays.* 7(4):176–178.

Young, C. L., F. S. Southwick, and A. Weber. 1990. Kinetics of the interaction of a 41-kilodalton macrophage capping protein with actin: promotion of nucleation during prolongation of the lag period. *Biochemistry.* 29: 2232–2240.

Young, C. L., A. Feierstein, and F. S. Southwick. 1994. Calcium regulation of actin filament capping and monomer binding by macrophage capping protein. *J. Biol. Chem.* 269:13997–14002.

Yu, F.-X., P. A. Johnston, T. C. Sudhof, and H. L. Yin. 1990. gCap39, a calcium ion- and polyphosphoinositide-regulated actin capping protein. *Science (Wash. DC).* 250:1413–1415.

Yu, F.-X., D.Zhou, and H. L. Yin. 1991. Chimeric and truncated gCap39 elucidate the requirements for actin filament severing and end capping by the gelsolin family of proteins. *J. Biol. Chem.* 266:19269–19275.

Yu, F.-X., H.-Q. Sun, P. A. Janmey, and H. L. Yin. 1992. Identification of a polyphosphoinositide-binding sequence in an actin monomer-binding domain of gelsolin. *J. Biol. Chem.* 267:14616–14621.

Yu, F.-X., S.-C. Lin, M. Morrison-Bogorad, and H. L. Yin. 1994. Effects of thymosin β4 and thymosin β10 on actin structures in living cells. *Cell Motil. Cytoskeleton.* 27:13–25.